



# Why does spatial extrapolation of the vine water status make sense? Insights from a modelling approach

Sébastien Roux, Rémi Gaudin, Bruno Tisseyre

## ► To cite this version:

Sébastien Roux, Rémi Gaudin, Bruno Tisseyre. Why does spatial extrapolation of the vine water status make sense? Insights from a modelling approach. *Agricultural Water Management*, 2019, 217, pp.255-264. 10.1016/j.agwat.2019.03.013 . hal-02609250

**HAL Id: hal-02609250**

**<https://hal.inrae.fr/hal-02609250>**

Submitted on 26 Oct 2021

**HAL** is a multi-disciplinary open access archive for the deposit and dissemination of scientific research documents, whether they are published or not. The documents may come from teaching and research institutions in France or abroad, or from public or private research centers.

L'archive ouverte pluridisciplinaire **HAL**, est destinée au dépôt et à la diffusion de documents scientifiques de niveau recherche, publiés ou non, émanant des établissements d'enseignement et de recherche français ou étrangers, des laboratoires publics ou privés.



Distributed under a Creative Commons Attribution - NonCommercial 4.0 International License

# Why does spatial extrapolation of the vine water status make sense? Insights from a modelling approach

Sébastien Roux<sup>1,\*</sup>, Rémi Gaudin<sup>2</sup>, Bruno Tisseyre<sup>3</sup>

1: MISTEA, INRA, Montpellier SupAgro, Univ Montpellier, Montpellier, France

2: SYSTEM, INRA, Montpellier SupAgro, CIRAD, Univ Montpellier, Montpellier, France

3: ITAP, INRA, IRSTEA, Montpellier SupAgro, Univ Montpellier, Montpellier, France

\*: corresponding author

## Abstract

This work is devoted to precision agriculture and more precisely to the spatial monitoring of water status in viticulture. An empirical approach was introduced in 2008 based on the extrapolation across a domain (vineyard block, vineyard, region) of vine water status observations from a reference site using a simple statistical model, called SPIDER, and proved efficient in many studies. Once the extrapolation model is calibrated, this approach leads to a concentration of measurements for one site only (reference site) while providing an estimate of the grapevine water status at a larger spatial scale. It is a promising hybrid approach based both on regular (but targeted) measurements and on modelling. However, so far only empirical guidelines for its practical use have been provided. Moreover, the limits of validity (spatial, temporal, etc.) of such an approach are not known.

This work intends to use a mechanistic model based on grapevine water balance modelling to study to what extent a simulated water status can be spatially extrapolated at the field scale. The water balance model was calibrated on two datasets (different cultivars and weather data) and used to analyse the performances of SPIDER. The results confirmed the relevance of the empirical approach (SPIDER) based on water status spatial extrapolation with a low error level on the two datasets studied. The use of the water balance model also helped define the validity domain of SPIDER: it confirmed the importance of having dominantly dry conditions and revealed the possibility of recovering good prediction quality after strong rainfall or irrigation. This study globally demonstrates the relevance of spatial extrapolation of the vine water status from a reference site with a

linear regression model and provides new insights on the properties of the predictions for application in viticulture either at the within-field level or at larger scale.

## 1. Introduction

Several studies have shown that changes in grapevine water status ( $\Psi$ ) have a direct effect on grape composition and quality by influencing vegetative growth, fruit growth, yield, canopy microclimate, and fruit metabolism (see among others, Tregoat et al., 2002; Dry and Loveys, 1998; Van Leeuwen and Seguin, 1994; Ojeda et al., 2002; Brillante et al., 2018). Characterizing the spatial variability of  $\Psi$  is then a key issue for terroir study (Seguin, 1983; Van Leeuwen et al., 2009). The spatial monitoring of  $\Psi$  therefore provides important information for managing and/or assessing grape quality (Van Leeuwen et al., 2009; Rezaei and Reynolds, 2010). In a review paper, Acevedo-Opazo et al. (2008) discussed the importance of methods for spatial monitoring of vine water status. Furthermore, the same authors proposed an empirical spatial model (Eq. 1) to predict the vine water status (estimated with the water potential  $\Psi$ ) across a given domain (vineyard block, vineyard, region, etc.).

$$\Psi(s, t) = a_s \cdot \Psi(s_{ref}, t) \quad [\text{Eq.1}]$$

The principle of the model is to extrapolate a reference  $\Psi$  value  $\Psi(s_{ref}, t)$  measured at a reference site  $s_{ref}$  and time  $t$ . The extrapolation is based on a linear relationship defined by the coefficients  $a_s$  whose values are specific to site  $s$ . The model provides an estimate  $\Psi(s, t)$  of  $\Psi$  values at any site  $s$  where a coefficient  $a_s$  is available. This spatial model has been successfully tested at the within-field level (Acevedo-Opazo et al., 2010) and at a vineyard level constituted of several blocks (Taylor et al., 2010). More recently, the model has been successfully tested at the whole denomination scale by Baralon et al. (2012). At this scale, the approach was called SPIDER (SPatial extrapolation of the vlne water status at the whole DENomination scale from a Reference site). Although empirical, The SPIDER approach may present several practical advantages: i) it relies solely on direct  $\Psi$  measurements (i.e. leaf water potential), which can be performed by vine growers. Therefore, the calibration of the model can be implemented within a conventional monitoring of  $\Psi$ . The method does not require spatial estimates of other variables related to soil or other environmental factors that may be difficult and expensive to measure; ii) the model can also be calibrated from measurements that have already been taken.

66 Therefore, it makes it possible to use existing databases of  $\Psi$  (historical databases),  
67 provided that the data are geo-located; and iii) the principle of the method allows to  
68 consider asynchronous measurements when labor is the limiting factor, provided that the  
69 measurement of  $\Psi$  is systematically done on the reference site.

70 Despite these practical advantages, the results obtained have highlighted a number of  
71 limitations of SPIDER that the empirical approach allows to observe but does not allow to  
72 quantify objectively. Two main limitations have been identified (Baralon et al., 2012); the  
73 first one refers to the climatic context of the year used to calibrate the model. Indeed,  
74 Baralon et al. (2012) stressed that the database used to calibrate the model must  
75 necessarily include data with a large magnitude of water restriction which requires a  
76 sufficiently long summer period without any rainfall to reach high  $\Psi$  values over the domain  
77 under consideration. The second limitation relates to conditions concerning the soil,  
78 climate and cultural practices that the study area must present so that the linear  
79 relationship associating  $\Psi$  from the reference site to  $\Psi$  of any site remains relevant (i.e.  
80 constant) over the time. For example, Taylor et al. (2010) showed that  $\Psi$  extrapolation  
81 appeared to be feasible between fields despite different soil types if the general soil  
82 moisture regimes were similar. Indeed, the linear relationships considered in the model did  
83 break down when the soil moisture regimes or when rainfall amounts were variable  
84 between the reference site and the site of prediction. Similarly, the linear relationship with  
85 the reference site may be altered by irrigation (Baralon et al., 2012).

86 Because SPIDER is based on a data-based learning approach, it provides a limited formal  
87 framework to explore these limitations. More specifically, it does not allow to study the  
88 effect of a differentiated water input (i.e. rainfall, irrigation) on the quality of the estimates  
89 produced by extrapolation from a reference site. For example, it is impossible to know if  
90 there is a critical precipitation level beyond which extrapolation can no longer be applied,  
91 in the same way it is difficult to know if the linear relationship is definitively lost for the  
92 season after a rainfall event or if it is again possible to apply the model after a sufficiently  
93 long dry period. Recent work (Gaudin et al., 2017) has shown that a mechanistic approach  
94 based on a Water Balance Model (WBM) can contribute to understanding within-field  
95 variations of the vine water status. These results suggest that such a modelling approach  
96 might be used to study the spatial extrapolation problem by simulating the water status  
97  $\Psi^{sim}(s, t)$  for several sites within the same field and by analysing how these simulated  
98 dynamics relate to the one corresponding to a reference site. The main objective of this  
99 paper is thus to use a vineyard dataset and a Water Balance Model to perform these  
100 analyses and to provide a new angle for studying the validity of SPIDER and its limitations.

101

102 The paper is organised in three parts: i) the first will present the calibration of the WBM  
103 with historical data and its validation, ii) the second will present implementation of the  
104 WBM to validate the SPIDER approach based on extrapolation of simulated  $\Psi$  values from  
105 a reference site and then iii) the last part will use WBM properties to better understand the  
106 validity of SPIDER especially in the case of water supply either by rainfall or irrigation.

107

## 108 **2. Material and Methods**

109

### 110 **2.1. Dataset of predawn water potential observations in a Mediterranean vineyard:** 111 **Shiraz2004 and Mourvèdre2005**

112 Over the last 20 years, year 2004 and to a lesser extent 2005, were identified as the best  
113 summer periods for this work. Indeed, in both these years, Languedoc experienced very  
114 long periods of dry conditions interrupted by significant rainfall events. Predawn leaf water  
115 potential data were collected in 2004 for one variety (Shiraz) and in 2005 for the other  
116 variety (Mourvèdre) by Acevedo-Opazo et al. (2010) in vineyards of Pech Rouge (INRA  
117 Gruissan, 43°08'47" N, 03°07'19" E). The 1.2 ha Shiraz vineyard was planted in 1990 (Fig.  
118 1). The 1.7 ha Mourvèdre vineyard was also planted in 1990. Both are included in the *la*  
119 *Clape* terroir which is classified as a designation of origin by the French authority. The  
120 northern limits of this terroir follow the lower course of the river Aude and the southern  
121 limits follow a former riverbed of the same river. The corresponding geological terrain is  
122 Cretaceous limestone, mainly constituted of thick *Orbitolina* deposits (Lepinasse, 1982).  
123 Over time, this geological material has given rise to heterogeneity in the pedological  
124 material.

125 Predawn leaf water potential measurements were carried out between 3 and 5 a.m. on  
126 vines located on 49 sites of the fields (Acevedo-Opazo et al., 2010). These sites were  
127 defined following a regular grid as presented in Fig. 1. Measurements were made with a  
128 pressure chamber (Scholander et al., 1965) at six dates either in 2004 or in 2005. The  
129 pressure chamber was a Plant Water Status Console, Model 3000 (Soil moisture  
130 Equipment Corp., Santa Barbara, California). One date-site data corresponds to the  
131 average of three measurements on three representative vines at one site. In order to  
132 perform measurements over the 49 sites in a short period of time, the following  
133 organization was used: Three technicians and researchers collected the leaves and

134 brought them to a researcher (the same person for Shiraz and Mourvèdre fields) in charge  
135 of measurements on the console.  
136 Climatic data (Fig. 2) were monitored by the Pech Rouge weather station located 100 m  
137 away from the Shiraz field (500 m away from the Mourvèdre field). These climatic data  
138 were used to record rainfall events and to compute the reference evapotranspiration ( $ET_0$ )  
139 according to Allen et al. (1998)

140

## 141 **2.2. The Spider approach for extrapolating the water status dynamics from reference** 142 **sites**

143

144 The SPIDER model was presented in Eq. 1. It was implemented on data collected in 2004  
145 and 2005. Its principle is based on the (random) choice of a reference site ( $s_{re}$ ). Available  
146  $\Psi$  data were used to calibrate a linear model linking the  $\Psi$  values of the reference site to  $\Psi$   
147 values of different sites in the domain. Once calibrated, as shown in Fig. 2, SPIDER can  
148 be used to extrapolate any measurements taken at the reference site to each site in the  
149 domain for which calibration was performed. This extrapolation uses a collection of  
150 coefficients ( $a_{s1}$ ,  $a_{s2}$ ,  $a_{s3}$ , ...,  $a_{si}$ ) specific to each site of the domain ( $s_1$ ,  $s_2$ ,  $s_3$ , ...,  $s_i$ ).

151

## 152 **2.3 The Water Balance Model (WBM) approach for simulating $\Psi$ dynamics**

153

### 154 **2.3.1 Vineyard water balance model**

155 Water balance simulation models applied to vineyards (Lebon et al., 2003; Celette et al.,  
156 2010) are used in many studies and particularly in Mediterranean conditions: i) to provide  
157 a diagnosis tool on vineyard water stress (Pellegrino et al., 2006), ii) to analyse the effect  
158 of intercropping between vine rows (Celette et al., 2010; Ripoche et al., 2010) or iii) to  
159 study irrigation needs (Gaudin and Gary, 2012; Roux et al., 2014). The main model output  
160 is the dynamics of a normalized water stress index based on soil water content and called  
161 Fraction of Transpirable Soil Water (FTSW). The principle of this approach is to compute  
162 the daily change in soil water content from different water fluxes that occur inside the soil  
163 volume accessible to vine roots. Adopting the modelling hypotheses used in Gaudin and  
164 Gary (2012), the resulting update of daily FTSW, noted  $FTSW_t$ , can be written as:

$$165 \quad FTSW_t = \min(1, \max(0, FTSW_{t-1} + \frac{1}{FTSW} (P_t - Q_t - E_t - T_t))) \quad [Eq.2]$$

166 In this model, the main daily water fluxes are:  $P_t$  (rain),  $Q_t$  (runoff),  $E_t$  (evaporation from  
167 bare soil) and  $T_t$  (vineyard transpiration). In Gaudin and Gary (2012),  $Q_t$  is computed using

168 the NRCS Curve Number method (NRCS, 2004), Et using the FAO method (Allen et al.,  
169 1998) and Tt as proposed by Lebon et al. (2003). The parameter TTSW is the Total  
170 Transpirable Soil Water content.

171 The link between the FTSW modelling approach and measurements of the vine water  
172 status based on predawn leaf water potential has been done by Lebon et al. (2003) and  
173 Pellegrino et al. (2005) who proposed an empirical relationship which appeared robust for  
174 several Mediterranean vineyard fields (Eq. 3).

$$175 \Psi \approx \Psi_{FTSW}(FTSW) = \max\left(-1.5, \frac{1}{b} \cdot \log\left(\frac{FTSW}{a}\right)\right), \text{ with } a = 1.0572, b = 5.3452 \text{ [Eq.3]}$$

176 Using Eq.2 and Eq.3 it is possible to simulate the dynamics of FTSW continuously and  
177 derive an estimation  $\Psi^{sim}(t)$  of water potential  $\Psi$  at time t. By limiting the simulation period  
178 to the stage of vine growth corresponding to full canopy development, only a few model  
179 inputs are required to implement Eq. 3. These inputs are presented in Table 1.

180

### 181 2.3.2. Calibration of the model on Shiraz2004 and Mourvèdre2005

182 In order to apply the WBM on the 49 sites of the two fields (Shiraz2004 and  
183 Mourvèdre2005), values for model parameters and input variables are requested. Weather  
184 variables ( $P_t$ ,  $ET_{0t}$ ) have been measured or derived from records from the weather station  
185 but other model inputs (TTSW, CN,  $k_{cb}$ , REW, TEW,  $\Psi^{sim}(0)$ ) have to be estimated using  
186 calibration from  $\Psi$  measurements. The following calibration procedure was considered:

187

188 **Step 1:** Definition of a set of plausible values for 4 unknown inputs (all except  
189 TTSW). The values selected for this work are presented in Table 2. The values in  
190 Table 2 were selected from expert knowledge. They correspond to quite  
191 representative values for the vineyards in the south of France and take into account  
192 the diversity of cases which it is possible to meet in this region.

193

194 **Step 2:** Estimation of  $k_{cb}/TTSW$  for each site of each field {Shiraz2004,  
195 Mourvèdre2005} using the following approach as proposed by Gaudin et al.  
196 (2017):

- 197 • Selecting measurements in dry conditions: dates {05/08, 18/08, 23/08} for  
198 Shiraz2004 and {23/06, 06/07, 19/07, 05/08} for Mourvèdre2005.
- 199 • Estimating the ratio  $k_{cb}/TTSW$  using the coefficient of the linear regression  
200 between  $\Psi^{obs}(t)$  and cumulated  $ET_0$  on the selected dry period.

201

**Step3:** Optimisation of parameters  $\{k_{cb}, REW, TEW, CN, \Psi^{sim}(0)\}$ :

- For each site  $i=1..49$  of each field {Shiraz2004, Mourvèdre2005}
- For each of the  $3*3*3*7=189$  combination values defined in Table 2
  - Computation of TTSW using  $k_{cb}/TTSW$  values as estimated in Step 2 and current  $k_{cb}$  value,
  - Computation of  $\Psi^{sim}(t)$  for each parameter combination using the WBM
  - Computation of the mean absolute error (MAE) between simulations and observations. The precise expression of  $MAE_i$  for  $n_{obs}$  observations taken at times  $(t_1^{obs}, \dots, t_{n_{obs}}^{obs})$  was obtained by comparing measurements  $\Psi_i^{obs,k} = \Psi_i^{obs}(t_k^{obs})$  and model predictions  $\Psi_i^{sim,k} = \Psi_i^{sim}(t_k^{obs})$  on a site “i” as indicated in Eq.4 :

$$MAE_i = \frac{1}{n_{obs}} \sum_{k=1}^{n_{obs}} |\Psi_i^{obs,k} - \Psi_i^{sim,k}| \quad [Eq.4]$$

- Selection of the set of parameters corresponding to the lowest MAE

Using this procedure, it was possible to obtain for each site “i” in each field: i) a continuous simulation of  $\Psi_i^{sim}(t)$  during the measurement period, ii) a quantification of the calibration error (here the Mean Absolute Error), iii) the set of optimized model parameters.

## **2.4. Methods for analysing the SPIDER approach using the Water Balance Model**

### **2.4.1. Assessment of calibration performances of the WBM**

In order to analyse the calibration performances of the WBM applied on the 49 sites of the two dataset Shiraz2004 and Mourvèdre2005,  $\Psi^{sim}(t)$  was computed for each site. The associated Mean Absolute Error of Calibration was then estimated using Eq. 4. For each field the distribution over all sites of the obtained MAE was then analysed.

### **2.4.2. Choice of the reference sites**

SPIDER requires the choice of a reference site in order to predict, for any site “i”, the value of the potential  $\Psi_i^{obs}(t_k)$  from the value observed on a reference site  $\Psi_{ref}^{obs}(t_k)$ . It has been shown in previous studies that SPIDER prediction performances were not very sensitive to the choice of the reference site (Acevedo et al., 2010; Baralon et al., 2012). It is however crucial for applying the WBM that the reference site is well adjusted by model simulations.



In order to take this constraint into account, for each field, the reference site was chosen by taking the site with best WBM calibration error among the best sites of reference for SPIDER. By applying this procedure to each field, site 29 and site 26 were selected as reference sites respectively for Shiraz and Mourvèdre.

### 2.4.3. Validating the global performances of SPIDER using WBM simulations

The performance of SPIDER is measured by the prediction error. This latter as well as the linear model are defined on a small number of available observations and may therefore be biased by the limited number of measurements.

Using the WBM, the linear regression between the continuous dynamics of a reference site  $\Psi_{ref}^{sim}(t)$  and the associated dynamics of a target site  $\Psi_i^{sim}(t)$  can be computed:  $\hat{\Psi}_i^{sim}(t) = a_i^{sim} \cdot \Psi_{ref}^{sim}(t)$ . It is therefore possible to test the prediction error of this model for each day within the measurement period. This prediction error can be seen as a generalization of the SPIDER prediction error as it also uses a linear regression model between  $\Psi$  values based on the use of a single reference site. This prediction is also more robust compared to the one based only on measurements in the sense that the number of samples is much higher (simulations are carried out every day in the measurement period). The SPIDER approach may be considered validated if the prediction errors obtained using continuous predictions of the WBM are low for most sites. In the rest of the document, the use of the data derived by the WBM to simulate the SPIDER approach as described in this section will be referred to as: WBM based regression.

### 2.4.4 Theoretical analysis of SPIDER performances using the WBM in dry conditions

SPIDER limitations were investigated using the WBM approach. From Gaudin et al. (2017), it is known that under dry conditions the plant water potential decreased linearly in relation to the cumulated  $ET_0$ . Moreover, the slope of this relation can be expressed using model parameters: it is equal to the ratio of  $k_{cb}$  (basal crop coefficient) to TTSW (Total Transpirable Soil Water).

It is therefore possible to understand how simulated  $\Psi$  dynamics at different sites in a same field are related during a dry period. More precisely, regarding a dry period starting at time  $t_0$ , Eq. 5 summarises changes in plant water potential for a reference site “ref” and a target site “i”.

$$\begin{aligned} \Psi_i^{sim}(t_0 + t) &= \Psi_i^{sim}(t_0) + \frac{k_{cb,i}}{TTSW_i} \sum_{s=t_0}^t ET_0(s) \\ \Psi_{ref}^{sim}(t_0 + t) &= \Psi_{ref}^{sim}(t_0) + \frac{k_{cb,ref}}{TTSW_{ref}} \sum_{s=t_0}^t ET_0(s) \end{aligned} \quad [Eq.5]$$

These equations will be combined to study the relationship between spatialized simulated water potentials in dry conditions.

### 3. Results and Discussion

#### 3.1. Calibration of WBM on historical $\Psi$ data

The cumulated density of calibration error of WBM is presented in Fig. 4. The error, defined as the Mean Absolute Error between observations and simulations and expressed in MPa, ranges from 0.03 MPa to 0.22 MPa and from 0.04 MPa to 0.25 MPa for Mourvèdre2005 and Shiraz2004 respectively. 80% of the sites have an error lower than 0.15 MPa for Mourvèdre2005 and lower than 0.18 MPa for Shiraz2004. For each field, two sites were highlighted in red in Fig. 4: sites 37 and 32 for Shiraz and sites 23 and 25 for Mourvèdre. These sites were chosen to encompass the large range of calibration errors from MAE = 0.05 MPa (site 37 and 23) to MAE = 0.15 MPa (sites 32 and 25). They are used in Fig. 5 to illustrate the evolution dynamics of the estimated plant water potential estimated from the WBM in contrasting situations (in terms of error) for the two fields. Fig. 5 shows a low error level of 0.05 MPa obtained on site 37 (Shiraz2004) and 23 (Mourvèdre 2005). Very well adjusted curves on almost all measurements are associated to this low error level. A moderate error level of 0.15 MPa is obtained on site 32 (Shiraz2004) and 25 (Mourvèdre2005). For such sites, the model does not adjust properly to all measurement dates. Higher deviations between outputs of the model and observed values are noticed at the beginning of the measurement period for site 32 (Shiraz2004) while over and under estimations are observed over the whole experimentation period for site 25 (Mourvèdre2005).

As seen in Fig. 4, the calibration is globally better on Mourvèdre2005 than on Shiraz2004, and overall these error levels are considered acceptable to use the model for the spatial extrapolation problem.

#### 3.2. Validation of the SPIDER model on historical $\Psi$ data

Fig. 6 shows a comparison between errors observed with SPIDER and WBM based regression. For Mourvèdre2005, the prediction error using the WBM-based regression is low (<0.15 MPa for 90% of sites) and close to error values obtained with SPIDER. For Shiraz2004, 80% of the sites have a prediction error lower than 0.15 MPa. (Note that the

remaining 20% are also characterized by higher calibration errors: the model does not adjust at its best and the WBM-based regression results are thus less significant on these sites.)

Overall, the prediction error of the WBM-based regression appears low for both fields. This means that the knowledge of the simulated  $\Psi$  dynamics on a reference site allows to predict with relatively high precision the simulated  $\Psi$  dynamics on a target site using the simple linear regression model  $\widehat{\Psi}_i^{sim}(t) = a_i^{sim} \cdot \Psi_{ref}^{sim}(t)$ . This result strengthens the validity of SPIDER: indeed, it shows that the linear regression model based on several  $\psi$  measurements (SPIDER) is also valid when considering simulated  $\Psi$  dynamics at any day within the measurement period. This is one significant result of the present paper.

Fig. 7 allows to analyse the results obtained with linear predictions from an observed or simulated reference site more precisely. It shows the simulated  $\Psi$  dynamics for two sites: sites 37 (Shiraz2004) and 23 (Mourvèdre2005). Both sites present a low calibration error (see Fig. 4) and a low prediction error using the WBM-based regression (0.11 MPa for site 37 and 0.03 MPa for site 23). The regression line (in grey) is therefore in both cases an accurate way to predict  $\Psi_i^{sim}(t)$  (grey circles) from  $\Psi_{ref}^{sim}(t)$ . It can be noted in Fig. 7 that while the linear model is a good approximation of the link between  $\Psi$  dynamics, this relationship may present some complex features: for site 23 (Mourvèdre2005), non-linearity is observed for low  $\Psi$  values. For site 37 (Shiraz2004) the relationship between  $\Psi$  values is mostly piecewise linear. Different correlations seem to apply at different periods with the same slope but different intercepts. These properties will be further analysed in the following section.

### 3.3. Theoretical analysis of SPIDER performances in dry conditions

The previous results have shown that the WBM approach was able to validate the SPIDER results on the two-year data set. This section aims at using the WBM in order to gain more insights into the SPIDER conditions of application. To this aim both dry and wet conditions were considered.

#### 3.3.1. Dry conditions: piecewise linearity

From Eq.5 and using the simple trick that  $ax + b = \frac{a}{c} \cdot (cx + d) + b - \frac{ad}{c}$  (for any  $c \neq 0$ ), the following relationship (Eq.6) between simulated  $\Psi$  values can be obtained under dry conditions:

$$\Psi_i^{sim}(t_0 + t) = \left( \frac{k_{cb,i} \cdot TTSW_{ref}}{k_{cb,ref} \cdot TTSW_i} \right) \Psi_{ref}^{sim}(t_0 + t) + \Psi_i^{sim}(t_0) - \left( \frac{k_{cb,i} \cdot TTSW_{ref}}{k_{cb,ref} \cdot TTSW_i} \right) \Psi_{ref}^{sim}(t_0) \quad [\text{Eq.6}]$$

Eq. 6 can be written as follows:

$$\Psi_i^{sim}(t_0 + t) = a_i^{param} \cdot \Psi_{ref}^{sim}(t_0 + t) + b_i^{param, t_0} \quad [\text{Eq.7}]$$

$$\text{with } \begin{cases} a_i^{param} = \left( \frac{k_{cb,i} \cdot TTSW_{ref}}{k_{cb,ref} \cdot TTSW_i} \right) \\ b_i^{param, t_0} = \Psi_i^{sim}(t_0) - a_i^{param} \cdot \Psi_{ref}^{sim}(t_0) \end{cases}$$

Eq.7 shows that every dry period starting at  $t=t_0$  results, for  $t>t_0$  and under dry conditions, in a linear relation between  $\Psi_i^{sim}(t)$  and  $\Psi_{ref}^{sim}(t)$ . The slope of this relation  $a_i^{param}$  is defined using basal crop coefficients and TTSW of each site and does not depend on the water status at  $t=t_0$ , unlike the intercept  $b_i^{param, t_0}$ . This property explains the piecewise linearity that can be seen in Fig.7a: there are clearly two periods of piecewise linearity in this simulation.

### 3.3.2. Persistent dry conditions: stable linearity

When dry conditions last a long time under high evaporative demand (high  $ET_0$ ), the model can be simplified. In such cases, the water potential reaches very low values and it is possible to neglect the influence of the intercept in the relationships between  $\Psi$  dynamics (Eq. 8).

$$\begin{aligned} \Psi_i^{sim}(t_0 + t) &= \Psi_i^{sim}(t_0) + \frac{k_{cb,i}}{TTSW_i} \sum_{s=t_0}^t ET_0(s) \approx \frac{k_{cb,i}}{TTSW_i} \sum_{s=t_0}^t ET_0(s) \\ \Psi_{ref}^{sim}(t_0 + t) &= \Psi_{ref}^{sim}(t_0) + \frac{k_{cb,ref}}{TTSW_{ref}} \sum_{s=t_0}^t ET_0(s) \approx \frac{k_{cb,ref}}{TTSW_{ref}} \sum_{s=t_0}^t ET_0(s) \end{aligned} \quad [\text{Eq.8}]$$

In these specific conditions, this implies that  $\Psi_i^{sim}(t_0 + t) \approx a_i^{param} \cdot \Psi_{ref}^{sim}(t_0 + t)$ . The linear relation is therefore mainly characterized by only basal crop coefficients and TTSW of each site, which is likely to be stable over several years.

### 3.3.3. Link between the regression coefficient and model parameters

Based on the previous section,  $a_i^{param}$  is known to drive the relationship between simulated  $\Psi$  dynamics during persistent dry conditions. In Fig. 8, a comparison between  $a_i^{param}$  and the regression coefficient  $a_i^{sim}$  of the predictive model using simulations (defined by  $\widehat{\Psi}_i^{sim}(t) = a_i^{sim} \cdot \Psi_{ref}^{sim}(t)$ ) is performed to evaluate if  $a_i^{param}$  can be a good estimate of  $a_i^{sim}$  even if the whole period does not correspond to dry conditions.

Both coefficients have been computed for each site in each field ( $a_i^{param}$  was computed from the calibrated model parameters,  $a_i^{sim}$  by linear regression on simulations).

Remember that 49 sites are available in each field. The site of reference being removed, this approach results in a comparison of 48 values for each field.

$a_i^{param}$  appears to be a good approximation of  $a_i^{sim}$  for both data sets Shiraz2004 and Mourvèdre2005 even if the weather conditions were not persistently dry (Fig. 8). On condition that  $k_{cb}$  and TTSW are stable over several years (which happens if the vine grower does not significantly change any management practices in the vineyard) and that climatic conditions are globally the same (dominantly dry), this implies that the linear relationship between simulated  $\Psi$  values should be globally stable over the years and related to model parameters  $k_{cb}$  and TTSW.

### 3.4. Impact of rainfall events on prediction quality in historical $\Psi$ data

The WBM approach allows to better study the limitation of SPIDER especially during and after a rainfall event or in case of irrigation. It should be noted that studying these situations is difficult with an empirical approach such as SPIDER since it would require performing a large number of measurements over limited periods of time. The implementation of an approach based on a validated WBM (under the conditions of the study) allows a more detailed study.

This analysis was made numerically on the two datasets using the methodology presented in Fig. 9 by focusing on the ratio of simulation  $\Psi$  dynamics for every  $t$  in the measurement period  $\frac{\Psi_i^{sim}(t)}{\Psi_{ref}^{sim}(t)}$  and on the regression coefficient  $a_i^{sim}$  derived from the WBM based regression ( $\widehat{\Psi}_i^{sim}(t) = a_i^{sim} \cdot \Psi_{ref}^{sim}(t)$ ). The normalized distance  $d_i(t)$  between this ratio of simulated  $\Psi$  and the regression coefficient was computed for each site  $i$  as is Eq.9:

$$d_i(t) = \frac{1}{a_i^{sim}} \cdot \left( \frac{\Psi_i^{sim}(t)}{\Psi_{ref}^{sim}(t)} - a_i^{sim} \right) \quad [\text{Eq.9}]$$

Finally, in order to aggregate the results for all sites, quantiles {10%,90%} of the  $d_i(t)$  distribution were computed. They are studied as a function of time to see how the local linearity between  $\Psi$  dynamics is broken by rainfall or irrigation events. Indeed, the periods where the linear approximation works well (resp. poorly) correspond to low (resp. high)  $d_i(t)$  values. Another point of interest is to look for recovery periods after a rainfall or irrigation event after which  $\Psi$  dynamics are again linearly correlated.

The assessment of the robustness of the linear approximation between  $\Psi$  dynamics is presented in Fig. 10. The prediction using a linear regression model has been shown to be

globally acceptable in Fig. 6, but it can be seen in Fig. 10 that rainfall alters the linearity of the relationship locally and that the interference is linked to the amount of rainfall. The impact of rainfall events is however not uniform even for a same amount of water: the heaviest rainfalls (for example the 20 mm rainfall on Shiraz2004) may not change the relationship for some sites while altering it for others. On the other hand, many small rainfall events (those  $<5$  mm) do not change the quality of the linear prediction, probably because the corresponding incoming water is evaporated very quickly. However, the main property stressed by Fig. 10 is the presence of a recovery time before regaining the previous quality of the linear model approximation, including after the heaviest rainfalls: the prediction using the linear model becomes accurate again after a certain time (see, for example, the 20 mm rainfall on Shiraz2004 and the decreasing of the error after this event).

This result is particularly significant and provides practical information for using an empirical approach like SPIDER. It shows that SPIDER could still be applied even after rainfall events or irrigation. After such events, there is transitory period during which any extrapolation of water status values observed on the site of reference would lead to biased estimations. However, SPIDER becomes relevant again after a certain period of time. For these experimentations, a period of 5 days would have been sufficient for most sites after a small rainfall event ( $<15$ mm) while a period of 15 days would have been required for heavier rainfall ( $>15$ mm). Naturally, further experiments will be necessary to validate this recommendation for its use on a larger scale.

420

## 4. Conclusion

422

This paper analyses why the vine water status, as characterized by predawn water potential values, can be extrapolated from measurements on a single reference site using a linear regression model known as the SPIDER approach. To perform this analysis, a water balance model running on a daily basis was used to provide daily estimates of predawn water potential values. The model was calibrated and used on two datasets (different vineyards, different years) with 49 sites of predawn leaf water potential measurements.

430

The use of the water balance model confirmed that predawn water potential values at any site can be estimated from observations performed on a reference site using a linear regression model linking the two dynamics with a low error level. For persistent dry

conditions occurring frequently in Mediterranean vineyards, the ratio of simulated predawn water potential values was shown to be simply linked to model parameters (basal crop coefficient and Total Transpirable Soil Water) indicating that the linear relationship between simulated water potential dynamics is stable over several years provided persistent dry conditions are dominant. Finally, the robustness of the relationship to rainfall or irrigation events was analysed using the water balance model. This demonstrated that the relationship between the simulated water potential dynamics is less predictive around a rainfall event but that its quality is recovered after a period of time if no other rain event occurs. This study demonstrates the relevance of spatial extrapolation of the vine water status from a reference site with a linear regression model with new insights on the properties of the predictions. This study confirms the interest of its application in viticulture either at the within-field level or at larger scale.

## 5. Acknowledgements

We thank Hernan Ojeda and Nicolas Saurin (INRA Gruissan) for sharing vineyards data.

## 6. References

- Acevedo-Opazo, C., Tisseyre, B., Ojeda, H., Ortega-Farias, S., Guillaume, S., 2008. Is it possible to assess the spatial variability of vine water status? *Journal International des Sciences de la Vigne et du Vin* 42(4), 203-219.
- Acevedo-Opazo, C., Tisseyre, B., Ojeda, H., Guillaume, S., 2010. Spatial extrapolation of the vine (*Vitis vinifera* L.) water status: A first step towards a spatial prediction model. *Irrigation Science* 28, 143-155.
- Allen, R.G., Pereira, L.S., Raes, D., Smith, M., 1998. Crop evapotranspiration. Guidelines for computing crop water requirements. Irrigation and drainage paper 56, FAO, Roma.
- Baralon, K., Payan, J.C., Salançon, E., Tisseyre, B., 2012. Spider: Spatial extrapolation of the vine water status at the whole denomination scale from a reference site. *Journal International des Sciences de la Vigne et du Vin* 46(3), 167-175.

467 Brillante, L., Mathieu, O., Lévêque, J., van Leeuwen, C., Bois, B., 2018. Water status and  
 468 must composition in grapevine cv. Chardonnay with different soils and topography and a  
 469 mini meta-analysis of the  $\delta^{13}\text{C}$ / water potentials correlation. Journal of the Science of Food  
 470 and Agriculture 98, 691-697.

471

472 Celette, F., Ripoche, A., Gary, C., 2010. WaLIS– A simple model to simulate water  
 473 partitioning in a crop association: The example of an intercropped vineyard. Agricultural  
 474 Water Management 97, 1749-1759.

475

476 Dry, P.R., Loveys, B.R., 1998. Factors influencing grapevine vigour and the potential for  
 477 control with partial rootzone drying. Australian Journal of Grape and Wine Research 4,  
 478 140-148.

479

480 Gaudin, R., Gary, C., 2012. Model-based evaluation of irrigation needs in Mediterranean  
 481 vineyards. Irrigation Science 30, 449-459.

482

483 Gaudin, R., Roux, S., Tisseyre, B., 2017. Linking the transpirable soil water content of a  
 484 vineyard to predawn leaf water potential measurements. Agricultural Water Management  
 485 182, 13-23.

486

487 Lebon, E., Dumas, V., Pieri, P., Schultz, H.R., 2003. Modelling the seasonal dynamics of  
 488 the soil water balance of vineyards. Functional Plant Biology 30, 679-710.

489

490 Lespinasse, P., 1982. Notice explicative de la feuille géologique Narbonne 1/50 000.  
 491 BRGM, Orléans.

492

493 NRCS, 2004. National Engineering Handbook. Chapter 10: Estimation of Direct Runoff  
 494 from Storm Rainfall.

495

496 Ojeda, H., Andary, C., Kraeva, E., Carbonneau, A., Deloire, A., 2002. Influence of pre- and  
 497 postveraison water deficit on synthesis and concentration of skin phenolic compounds  
 498 during berry growth of *Vitis vinifera* cv. Shiraz. American Journal of Enology and Viticulture  
 499 53, 261-267.

500

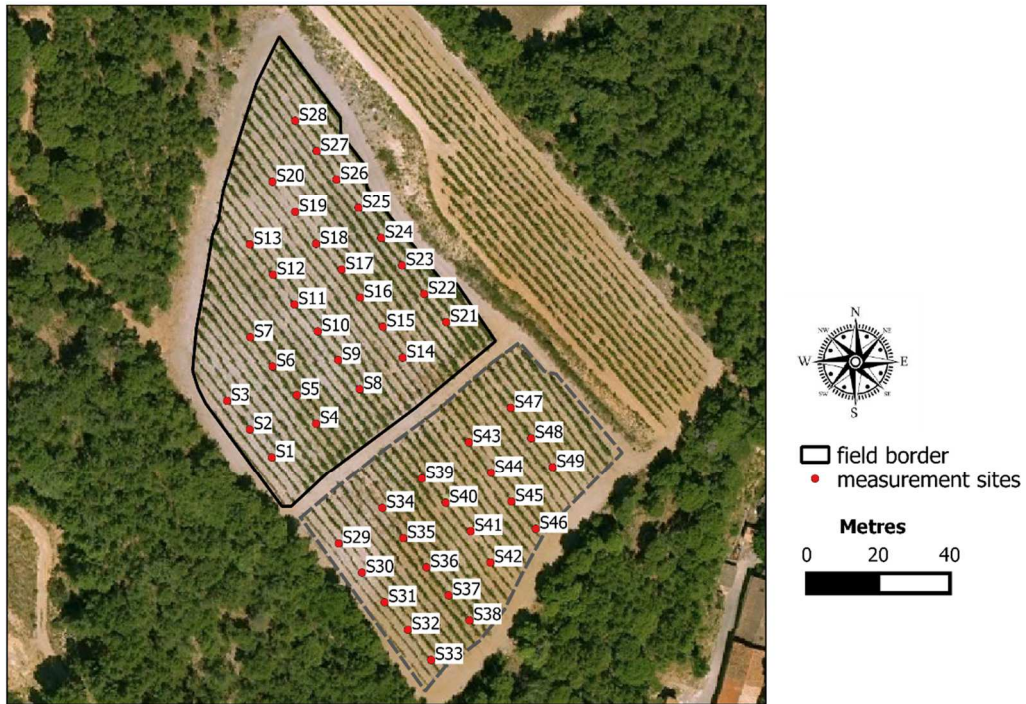


501 Pellegrino, A., Lebon, E., Simonneau, T., Wery, J., 2005. Towards a simple indicator of  
 502 water stress in grapevine (*Vitis vinifera* L.) based on the differential sensitivities of  
 503 vegetative growth components. Australian Journal of Grape and Wine Research 11, 306-  
 504 315.  
 505  
 506 Pellegrino, A., Gozé, E., Lebon, E., Wery, J., 2006. A model-based diagnosis tool to  
 507 evaluate the water stress experienced by grapevine in field sites. European Journal of  
 508 Agronomy 25, 49-59.  
 509  
 510 Rezaei, J.H., Reynolds, A.G., 2010. Impact of vine water status on sensory attributes of  
 511 Cabernet franc wines in the Niagara peninsula of Ontario. Journal International des  
 512 Sciences de la Vigne et du Vin 44(6), 61-75.  
 513  
 514 Ripoche, A., Celette, F., Cinna, J.P., Gary, C., 2010. Design of intercrop management  
 515 plans to fulfil production and environmental objectives in vineyards. European Journal of  
 516 Agronomy 32, 30-39.  
 517  
 518 Roux, S., Delpuech, X., Daudin, G., Brun, F., Wery, J., Wallach D., 2014. Providing user  
 519 oriented uncertainty information with a vineyard model used for irrigation decisions.  
 520 Volume 6 of the Advances in Agricultural System Modeling. Pract. Appl. Agric. Syst.  
 521 Models Optim. Use Ltd. Water, 5 (2014), pp. 183-208  
 522  
 523 Scholander, P.F., Hammel, H.T., Bradstreet, E.D., Hemmingsen, E.A., 1965. Sap  
 524 pressure in vascular plants. Science 148, 339-346.  
 525  
 526 Séguin, G. 1983. Influence des terroirs viticoles sur la constitution et la qualité des  
 527 vendanges. Bulletin de l'O.I.V. 56, 3-18.  
 528  
 529 Taylor, J.A., Acevedo-Opazo, C., Ojeda, H., Tisseyre, B., 2010. Identification and  
 530 significance of sources of spatial variation in grapevine water status. Australian Journal of  
 531 Grape and Wine Research 16, 218-226.  
 532  
 533 Tregoat, O., Van Leeuwen, C., Choné, X., Gaudillère, J.P., 2002. Etude du régime  
 534 hydrique et de la nutrition azotée de la vigne par des indicateurs physiologiques. Influence

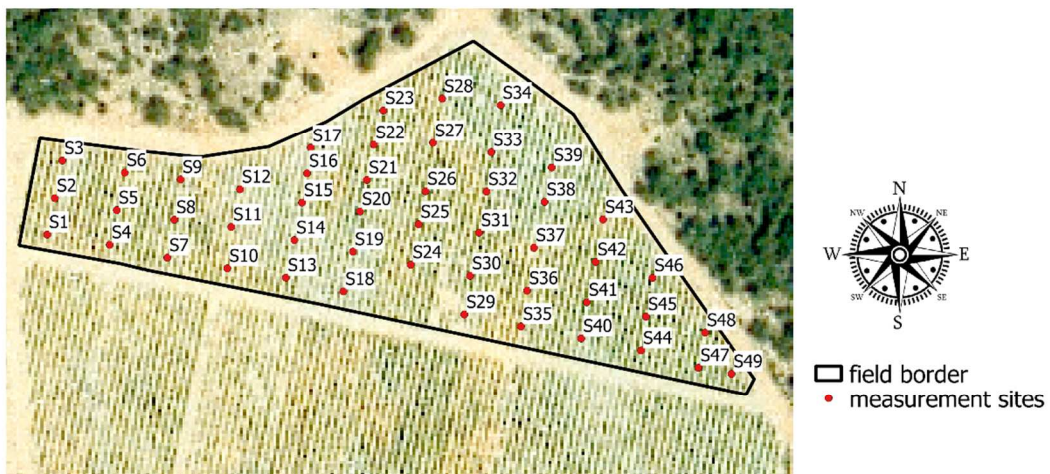
535 sur le comportement de la vigne et la maturation du raisin (*Vitis vinifera* L. cv Merlot,  
536 2000, Bordeaux). Journal International des Sciences de la Vigne et du Vin 36(3), 133-142.  
537

538 Van Leeuwen, C., Seguin, G., 1994. Incidences de l'alimentation en eau de la vigne  
539 appréciée par l'état hydrique du feuillage sur le développement végétatif et la maturation  
540 du raisin (*Vitis vinifera* variété Cabernet franc, Saint-Emilion 1990). Journal International  
541 des Sciences de la Vigne et du Vin 28(2), 81-110.  
542

543 Van Leeuwen, C., Tregoat, O., Choné, X., Bois, B., Pernet, D., Gaudillère, J.P., 2009. Vine  
544 water status is a key factor in grape ripening and vintage quality for red Bordeaux wine.  
545 How can it be assessed for vineyard management purposes? Journal International des  
546 Sciences de la Vigne et du Vin 43(3), 121-134.  
547  
548  
549  
550



a)



b)

**Fig. 1.** Map of Shiraz (a) and Mourvèdre (b) fields and their 49 measurement sites (Pech Rouge, INRA Gruissan, 43°08'47" N, 03°07'19" E).

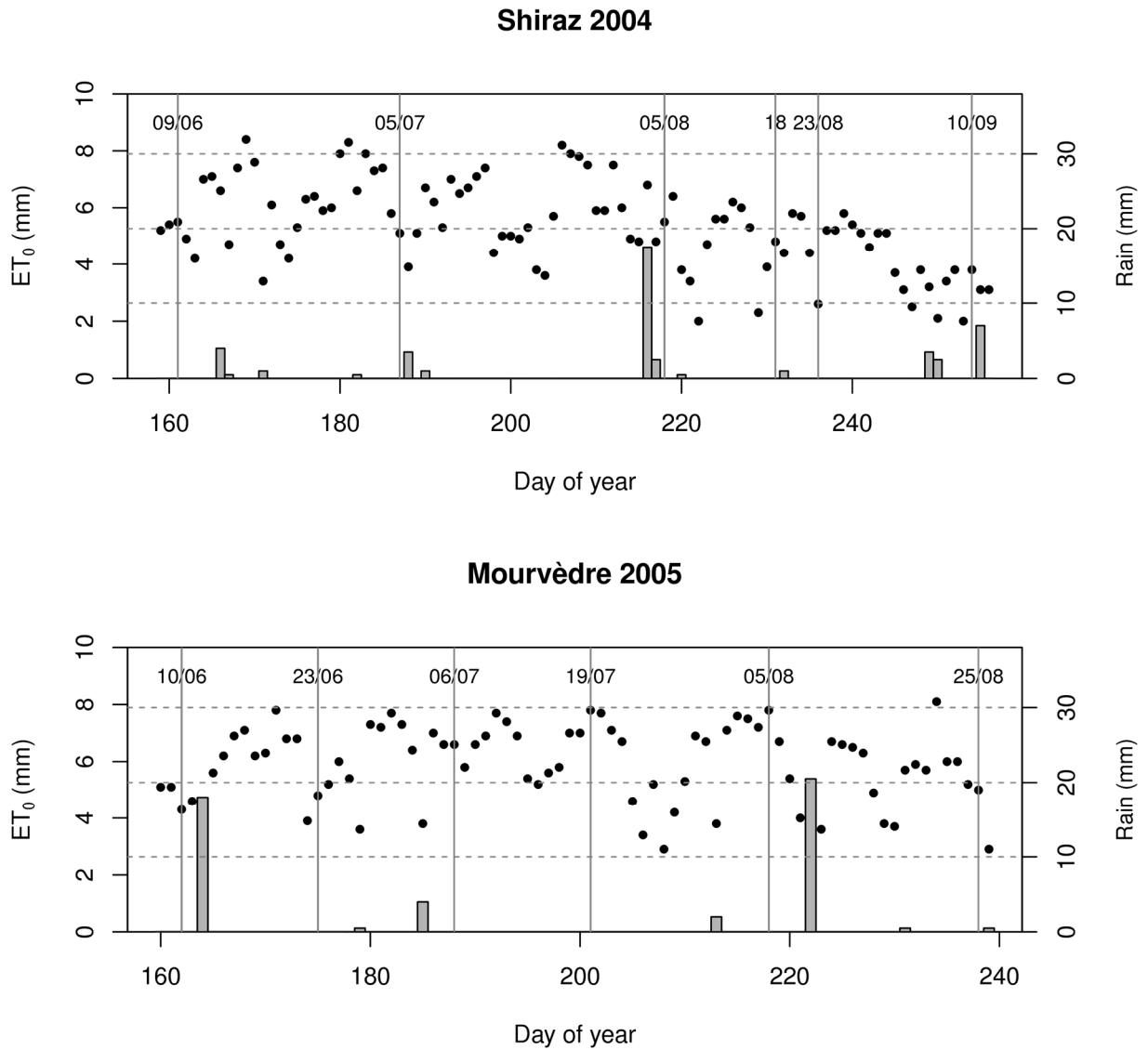


**Fig. 2.** Climatic data: Rainfall (grey bars) and Evapotranspiration (black dots) measured on the two fields Shiraz 2004 and Mourvèdre 2005 respectively between June-September 2004 and June-September 2005. Measurement dates of Predawn leaf water potential are indicated as vertical lines for each field.

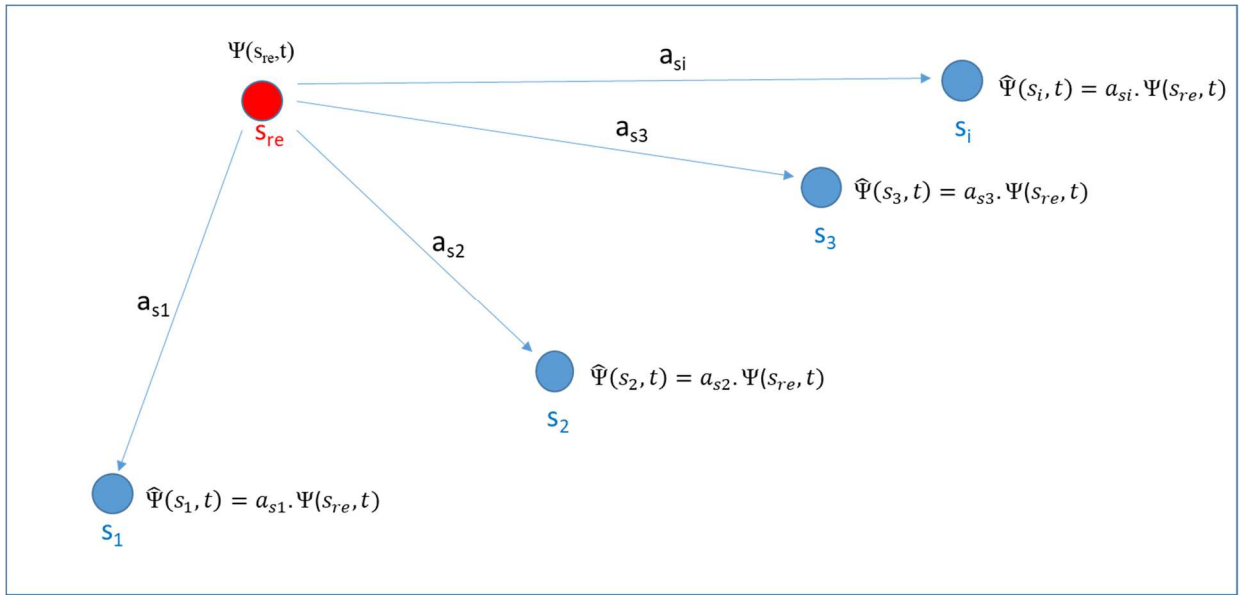


**Fig. 3.** The principle of the empirical approach SPIDER where the plant water potential ( $\Psi(s_{re}, t)$ ) measured at a reference site is linearly extrapolated to other locations ( $s_1, s_2, s_3, \dots, s_i$ ) of the field using site-specific coefficients ( $a_{s1}, a_{s2}, a_{s3}, \dots, a_{si}$ ) to provide estimates of plant water status ( $\Psi(s_1, t), \Psi(s_2, t), \Psi(s_3, t), \dots, \Psi(s_i, t)$ ) on unsampled locations at the same date  $t$ .

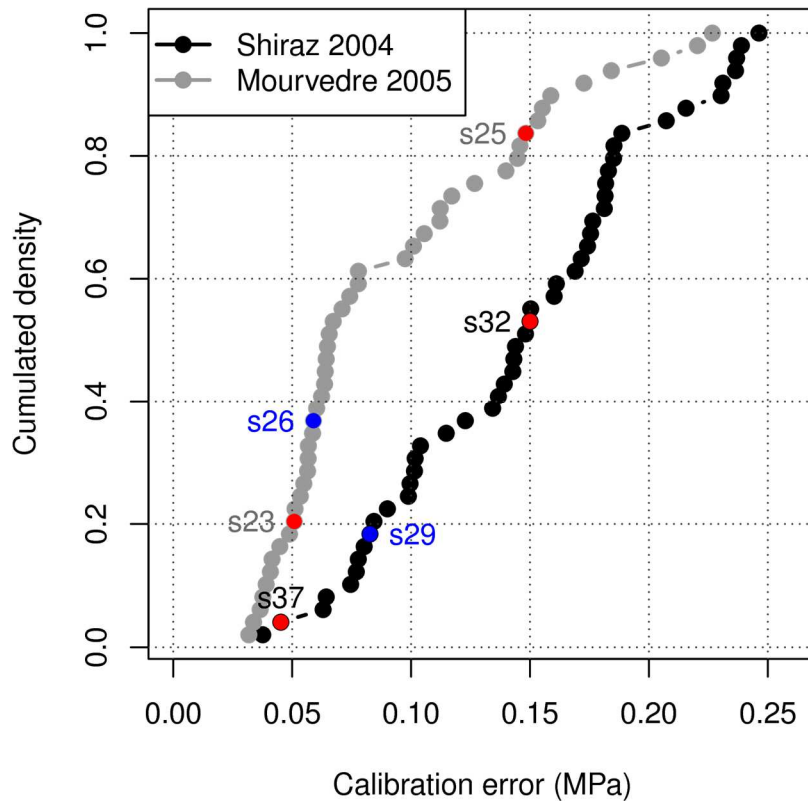


**Fig. 4.** The cumulative distribution of calibration errors (Mean Absolute Errors) of the model on the 49 sites in the two fields (sites in red are subjected to more detailed analysis presented in Fig. 5, and sites in blue are reference sites)

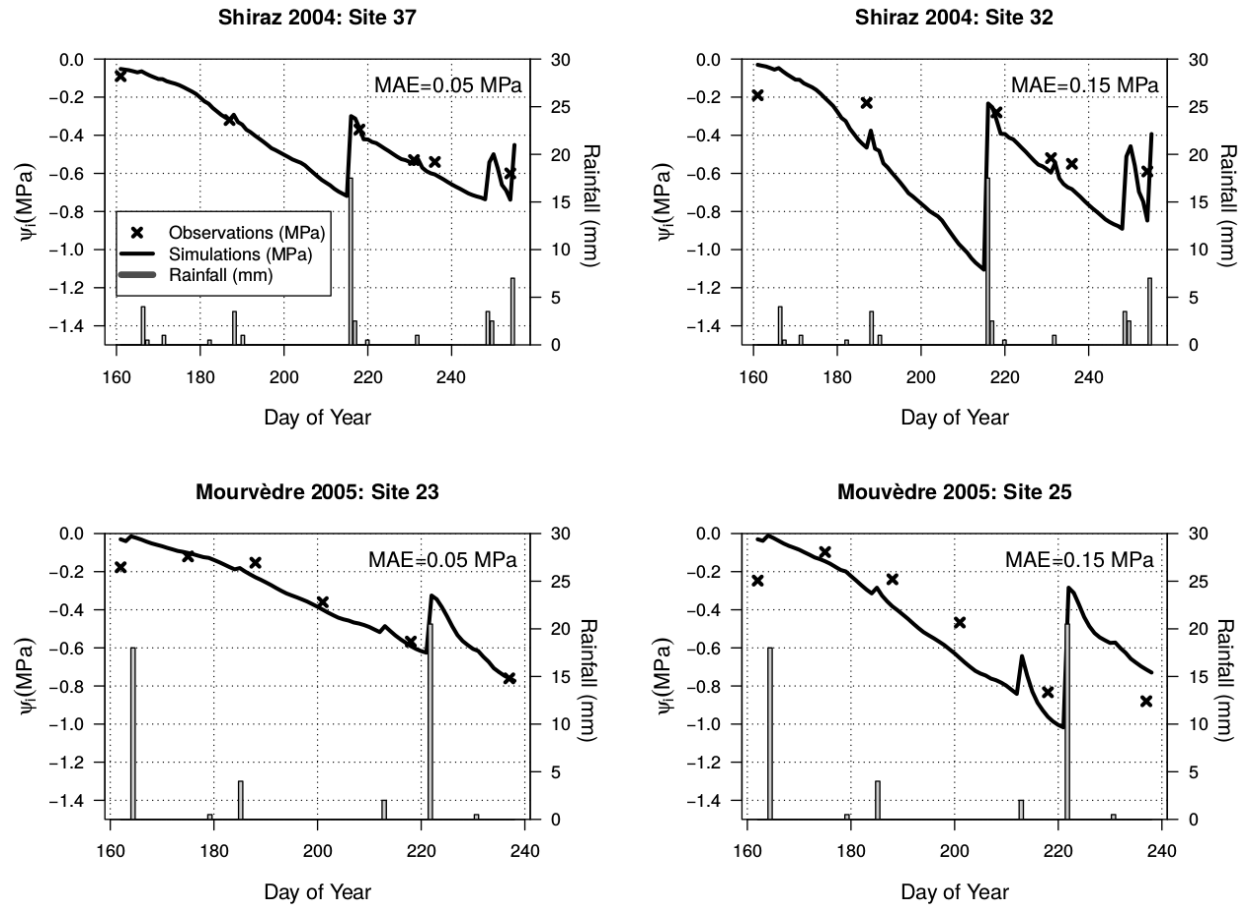


**Fig. 5.** Detailed analysis of the water balance model showing estimated and observed  $\Psi$  values for 2 sites of each field Shiraz2004 and Mourvèdre 2005. Sites were chosen to encompass the large range of calibration errors from MAE =0.05 MPa (site 37 and 23) to MAE = 0.15 MPa (sites 32 and 25).

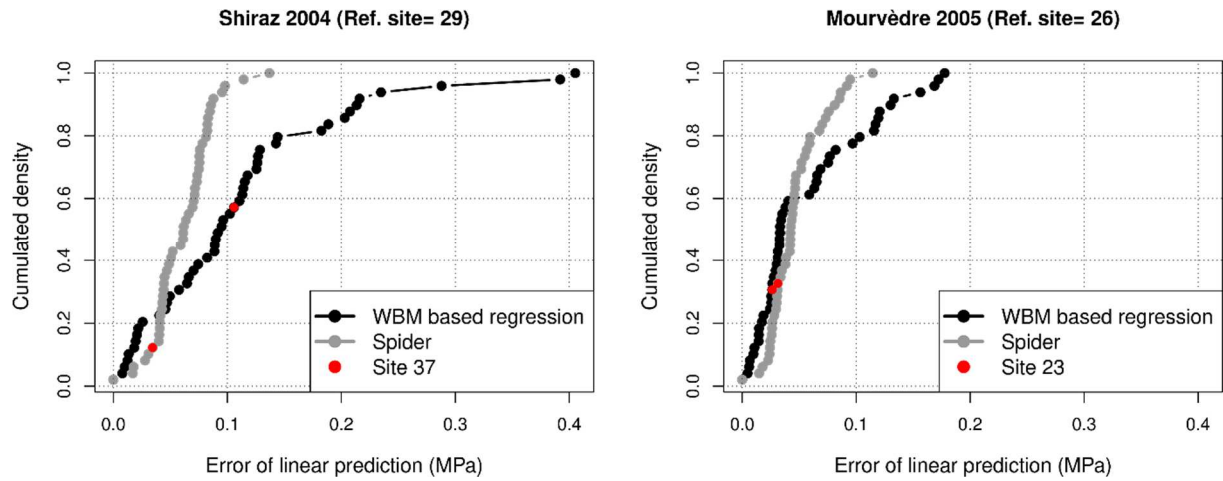


**Fig. 6.** Cumulative distribution errors (Mean Absolute Errors of Prediction, MPa) for SPIDER and for the WBM based regression. Result obtained on field Shiraz2004 are presented on the left and those obtained on Mourvèdre2005 on the right (the two sites are more precisely analysed in Fig. 7).



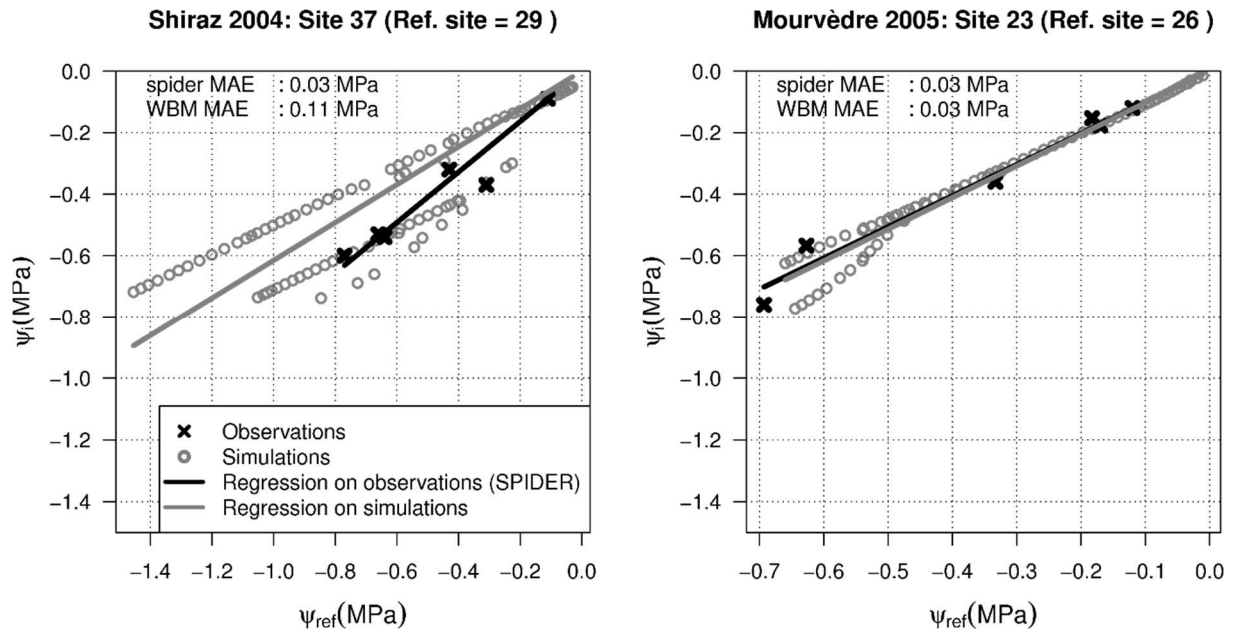


**Fig. 7.** The comparison of predictions obtained from a reference site with SPIDER and with the WBM-based regression for two sites.

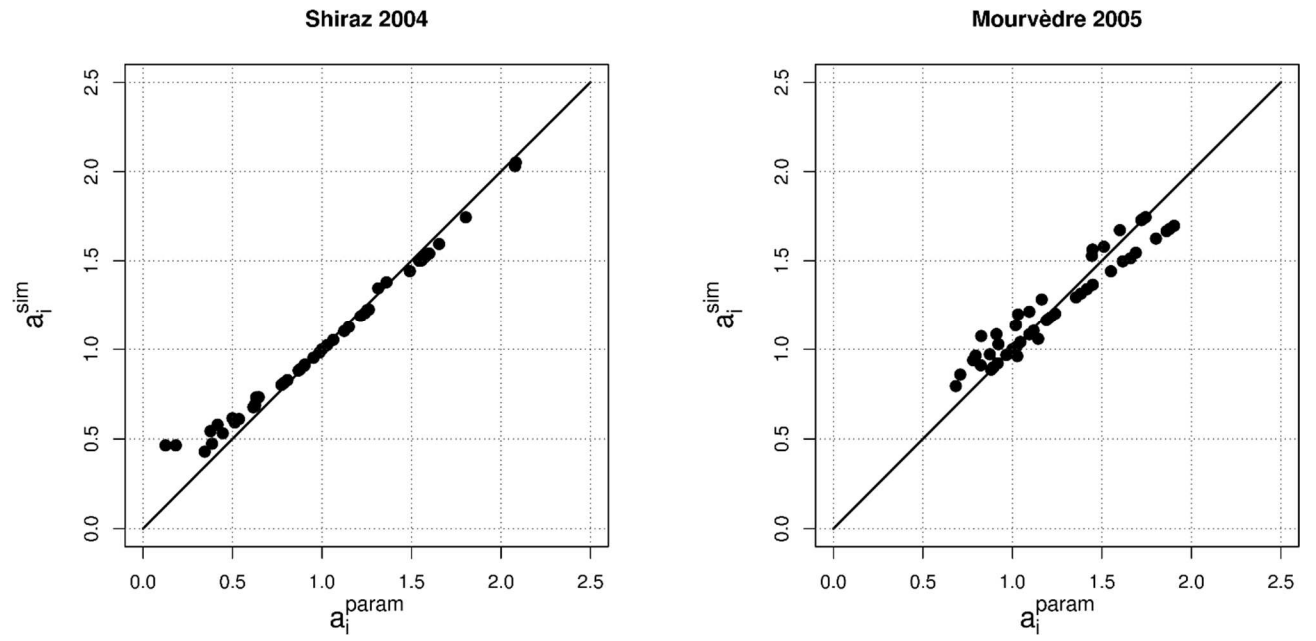


**Fig. 8.** The comparison of  $a_{sim}^i$  (coefficient of the WBM based regression) and  $a_i^{param}$  (derived from the WBM parameters  $k_{cb}$  and TTSW).

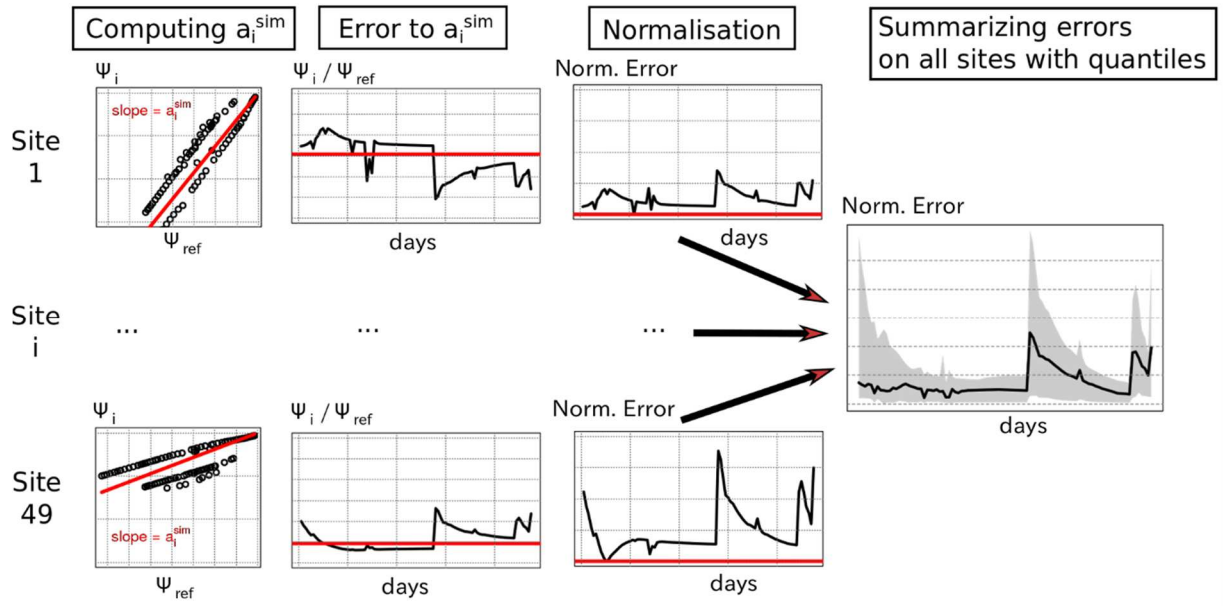


**Fig. 9.** Methodology used to analyse the impact of rain events on the quality of linear predictive model  $\hat{\Psi}_i^{sim}(t) = a_i^{sim} \cdot \Psi_{ref}^{sim}(t)$ . First the regression coefficients  $a_i^{sim}$  are computed, then an error is defined between the ratio of water potentials and the regression coefficient. This error is normalized in order to study its quantiles when aggregating the results on all 49 sites. The final results obtained for each field are presented in Fig. 10 and linked to climatic data.

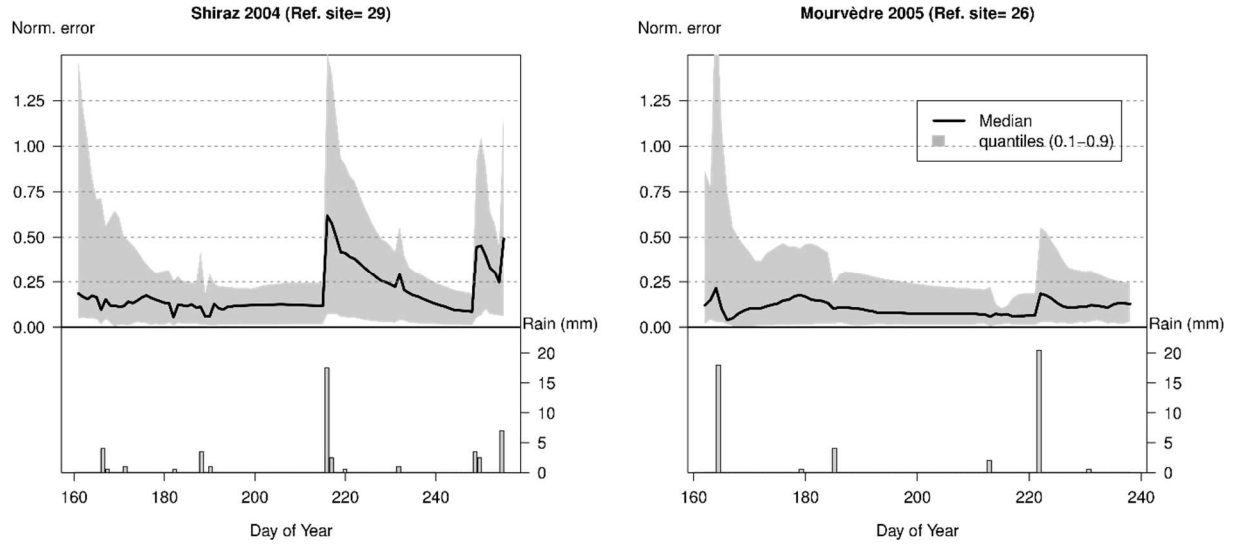


**Fig. 10.** Analysis of the temporal quality of the linear predictive model  $\hat{\Psi}_i^{sim}(t) = a_i^{sim} \cdot \Psi_{ref}^{sim}(t)$  using the quantiles of the normalized error  $d_i(t) = \frac{1}{a_i^{sim}} \left( \frac{\Psi_i^{sim}(t)}{\Psi_{ref}^{sim}(t)} - a_i^{sim} \right)$ . The median (in black) and quantiles (in grey) of the distribution of distances are plotted against time along with the distribution of rainfall.

Table 1: Water Balance Model inputs when limiting simulation to the full canopy development stage

Model Input name	Type of input	Definition	Unit
$\Psi^{sim}(0)$	Initial state	Vine water potential at simulation start	MPa
TTSW	Parameter	Total Transpirable Soil Water	mm
K <sub>cb</sub>	Parameter	Basal crop coefficient	-
CN	Parameter	Curve Number for runoff module	-
(REW,TEW)	Parameter	Readily and Total evaporable water	(mm,mm)
ET <sub>0t</sub>	input variable	Daily reference evapotranspiration	mm
P <sub>t</sub>	input variable	Daily rain	mm

Table 2: domain definition of the set of tested values for four model parameters

Parameter	Tested values
$k_{cb}$	$\{0.45; 0.5; 0.55\}$
$(REW, TEW)$	$\{(3,7); (5,12); (9,20)\}$
CN	$\{70, 80, 90\}$
$\Psi^{sim}(0)$	$\{\Psi_{FTSW}(0.3), \Psi_{FTSW}(0.4), \dots, \Psi_{FTSW}(0.9)\}$